Coupling between Rydberg States and Landau Levels of Electrons Trapped on Liquid Helium

K. M. Yunusova,[1,2] D. Konstantinov,[3] H. Bouchiat,[1] and A. D. Chepelianskii[1]
[1]LPS, Université Paris-Sud, CNRS, UMR 8502, F-91405 Orsay, France
[2]Institute of Physics, Kazan Federal University, Kazan 420008, Russian Federation
[3]Okinawa Institute of Science and Technology (OIST) Graduate University, Onna, Okinawa 904-0412, Japan

(Received 2 November 2018; revised manuscript received 5 February 2019; published 3 May 2019)

We investigate the coupling between Rydberg states of electrons trapped on a liquid helium surface and Landau levels induced by a perpendicular magnetic field. We show that this realizes a prototype quantum system equivalent to an atom in a cavity, where their coupling strength can be tuned by a parallel magnetic field. We determine experimentally the renormalization of the atomic transition energies induced by the coupling to the cavity, which can be seen as an analog of the Lamb shift. When the coupling is sufficiently strong, the transition between the ground and first excited Rydberg states splits into two resonances corresponding to dressed states with vacuum and one photon in the cavity. Our results are in quantitative agreement with the energy shifts predicted by the effective atom in a cavity model where all parameters are known with high accuracy.

DOI: 10.1103/PhysRevLett.122.176802

The realization of high purity two-dimensional electron systems (2DES) has led to the discovery of fundamental new states in condensed matter physics, like integer and fractional quantum Hall effects [1–5], as well as to the more recent discovery of two-dimensional topological insulators [6]. Electrons on liquid helium were one of the first historical realizations of the 2DES [7–10]. This system is formed due to the attractive interaction between electrons and their image charge inside liquid helium; it achieves an exceptional purity and still gives the best known electronic mobilities for a 2DES [11]. Electrons on helium enabled the first observation of Wigner crystallization [12,13], edge magnetoplasmons [14], and other exciting many-electron phenomena [15–19]. Considerable efforts were also devoted to study the interaction between electrons on helium and millimeter-wave photons aiming for applications in quantum computing [20,21]. This research direction recently revealed a rich nonequilibrium physics, showing microwave-induced oscillations (MIRO) [22–26], zero-resistance states [27–29], and incompressible electronic behavior [30–32] under excitation by millimeter-wave photons. In the present Letter, we show that electrons on helium also allow us to realize a model system for an atom interacting with an oscillator (cavity) and to explore its physical properties, directly controlling their coupling with a parallel magnetic field. Such systems have been embodied, for example, in atomic physics [33] and quantum optics, as well as with superconducting circuits [34,35]. We demonstrate that, for weakly coupled electrons, the quantum electrodynamics (QED) Hamiltonian reproduces quantitatively the spectroscopic properties of our system. This opens a doorway to study quantum phenomena in an ensemble of interacting atoms in a cavity system by tuning the strength of electron-electron interactions.

Before presenting our experimental results, we describe the derivation of the QED Hamiltonian for electrons on helium. The electric field of an electron polarizes the liquid helium around it and creates an image charge that attracts it towards the helium surface; a steep electron-volt high energy barrier prevents it from penetrating inside the liquid helium. The interaction with the image charge gives rise to a one-dimensional Coulomb potential, which leads to the quantization of the vertical motion and to the formation of a Rydberg series of bound states for a one-dimensional hydrogenlike atom. This series will play the role of the atomic degree of freedom in our QED model. A pressing perpendicular static electric field $E_\perp$ is also present in the experiments, it allows us to shift the Rydberg levels through the linear Stark effect [36]. The spectroscopic positions of the Rydberg states is well described by a one-dimensional Schrödinger equation for vertical motion,

$$\mathcal{H}_a = -\frac{\hbar^2}{2m}\frac{\partial^2}{\partial z^2} + V_a(z) = \sum_\alpha \varepsilon_\alpha |\alpha\rangle\langle\alpha|, \qquad (1)$$

where we introduced z as the vertical distance of the electrons to the helium surface, the eigenstates for the vertical motion $|\alpha\rangle$, and their eigenenergies ϵ_α. Above the helium surface, for $z > 0$, the confinement potential $V_a(z)$ is the sum of the interaction with the image charge and with the perpendicular electric field $V_a^0(z) = -\Lambda/z - eE_\perp z$ with $\Lambda = [e^2(\varepsilon - 1)/16\pi(\varepsilon + 1)]$

and where ε is liquid helium's dielectric constant. On the energy scale of the bound states (~7 K), we can set $V_a(z) = \infty$ inside liquid helium for $z < 0$. We introduced a subscript $V_a^0(z)$ to the potential since we will show later that $V_a(z)$ is renormalized when an in-plane magnetic field is present. For usual pressing electric fields $E_\perp \sim 2$ V mm^{-1}, the main contribution to the confinement potential for the lowest eigenstates comes from the interaction with the image charge.

In addition to their vertical motion, electrons on helium move horizontally as free particles—electrons with their bare electronic mass m. A perpendicular magnetic field applied to 2DES induces the Landau quantization of horizontal motion and the formation of equidistant Landau levels, and the Hamiltonian for horizontal motion (up to a constant) then becomes $\mathcal{H}_l = \hbar\omega_c \hat{a}^+\hat{a}$, where $\omega_c = eB_z/m$ is the cyclotron frequency. This term has the same form as the Hamiltonian of a resonant cavity in QED. The Landau level index then plays the role of the number of light quanta in the cavity. With only a perpendicular magnetic field and in the limit of weak electron-electron interaction, the Landau levels and Rydberg states are not coupled. A tunable coupling can be introduced by applying an in-plane magnetic field [37,38]. Indeed a magnetic field applied in the y direction will tend to turn a vertical velocity towards the x direction due to cyclotron motion along the y axis induced by the parallel field. This coupling has been investigated in double quantum wells in a regime with many occupied Landau levels [39–41]. In this Letter, we focus instead on the limit where only the lowest Landau level is occupied. The quantitative form of the interaction induced by the in-plane field can be obtained as follows. We write the total Hamiltonian $\mathcal{H} = [(\mathbf{p} - e\mathbf{A})^2/2m] + V_a^0(z)$, using the Landau gauge $\mathbf{A} = B_y z\mathbf{e}_x + B_z x\mathbf{e}_y$, where the vector potential does not have any component along the z axis motion. This Hamiltonian can be expanded in the powers of B_y: to the lowest order, we have $\hat{H} = \hat{H}_a + \hat{H}_l$. The first order in B_y introduces an atom-cavity interaction term $\hat{H}_c = -eB_y z\hat{p}_x/m$. Writing $\hat{H}_c$ in terms of the Landau level creation and annihilation operators, we obtain the following expression:

$$\hat{\mathcal{H}} = \hbar\omega_c \hat{a}^+\hat{a} + \sum_\alpha \varepsilon_\alpha |\alpha\rangle\langle\alpha| + \frac{\hbar\omega_y}{\sqrt{2}}(\hat{a}^+ + \hat{a})\frac{\hat{z}}{\ell_B}. \quad (2)$$

In this equation, we introduced the cyclotron frequency along the in-plane field $\omega_y = eB_y/m$, as well as the magnetic length for the perpendicular field $\ell_B = \sqrt{\hbar/(m\omega_c)}$. The notation $\hat{z}$ stands for the matrix elements of the z operator on the vertical eigenstates $|\alpha\rangle$. It plays here the role of the dipole moment operator in quantum electrodynamics. The QED Hamiltonian (2) appears in models where a photon mode (harmonic oscillator, Landau levels in our experiment) is coupled to an atom (qubit) provided by Rydberg states. The strength of the interaction, which would be the vacuum Rabi splitting in atomic physics, is directly controllable and proportional to B_y, allowing, in principle, couplings of arbitrary strength.

This Hamiltonian may seem valid to first order in B_y; however, the second-order diamagnetic term $m\omega_y^2 z^2/2$ only renormalizes the vertical confinement potential $V_a(z) = V_a^0(z) + m\omega_y^2 z^2/2$. Thus, Eq. (2) remains valid for arbitrary interaction strength, keeping in mind that the in-plane magnetic field then not only controls the coupling strength between the atom and Landau levels, but also changes the atom energies ϵ_α and the dipole momentum matrix $\hat{z}$, which can still be obtained easily by solving the one-dimensional Schrödinger equation (1) in the modified confinement potential.

To check if the QED Hamiltonian quantitatively describes the energy of the transitions between Rydberg states, we perform Stark effect spectroscopy. Electrons on helium form a static dipole with their image charge, and the Stark effect due to the perpendicular electric field $E_\perp$ leads to a linear displacement of the Rydberg energy levels, which can bring these atomic transitions in resonance with the external millimeter-wave excitation. At resonance, a change of resistivity occurs due to MIRO, allowing us to detect the position of the energy levels. Our experimental setup consists of a cavity with Corbino electrodes, the layout of which is shown in Fig. 1. This cavity is half filled with liquid helium by condensing helium vapor and

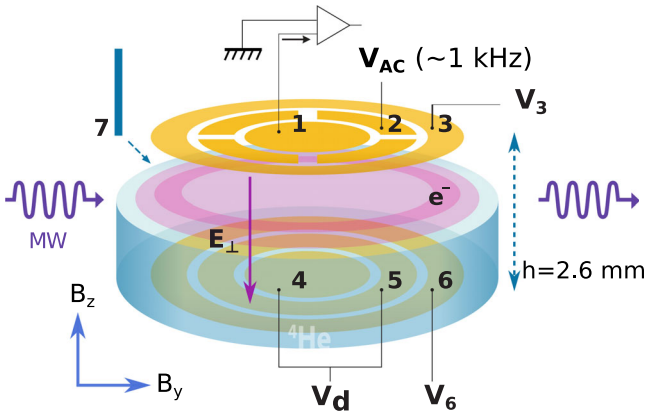

FIG. 1. Schematic diagram of the experimental cell. The top electrodes 1 and 2 are dc grounded and are used for the ac measurements. A positive dc voltage V_d is applied to electrodes 4 and 5, confining the electrons into the center of the cell and fixing $E_\perp = V_d/h$. Electrodes 3 and 6 are used as a guard with negative potential. To ensure an homogeneous $E_\perp$, we fixed $V_6 - V_3$ to V_d (and $V_d - V_6 = 6$ V). The admittance Y of the cell is obtained by applying a 10 mV ac voltage at 1137 Hz to the segmented electrode 2 and measuring the induced pickup voltage on electrode 1 with a lock-in amplifier. It depends on the in-plane conductivity of the electrons under magnetic field as obtained from Corbino measurements with Ohmic contacts on conventional 2DES. Microwave (MW) power was sent into the cell through a waveguide and electrode 7 is the filament (e^- source).

monitoring the capacitance between top and bottom electrodes. Electrons are then deposited by thermal emission from a heated filament and are trapped on the surface by the pressing electric field $E_\perp$. They form a 2DES that behaves, for in-plane transport, as an effective resistance R placed between two contacts with capacitance C. This resistance can then be determined by measuring the admittance of the cell Y between the two inner Corbino contacts from the top electrodes at frequencies comparable with the RC relaxation time (we used 1137 Hz). To extract the MW-dependent (MIRO) admittance δY, MW power is modulated at a frequency of 17 Hz and a double demodulation technique is used. Real and imaginary parts of δY give very similar line shapes. In our measurements, the electron gas density was $n_e \simeq 1.5 \times 10^7$ cm^{-2}, with a total number of 4×10^7 electrons trapped in the cloud.

The conversion between Stark shifts and transition energies is obtained from a calibration experiment where we excite the electrons with photons at different energies and measure the electric field at resonance (see Fig. 2). For weak parallel magnetic fields, the transition from the ground $|g\rangle$ to the first excited Rydberg state $|e\rangle$ manifests as a resonance of the microwave-induced change in admittance as function of $E_\perp$. The resonance position at energy $h\nu_0 = \epsilon_e - \epsilon_g$ shifts linearly with $E_\perp$, and the slope can be obtained from the Schrödinger equation (1) with small deviations due to uncertainties on geometrical parameters. This slope is almost independent of B_y [see Fig. 2(a)]; indeed, for $B_y \leq 1$ T, the coupling term of the QED Hamiltonian $(\hbar\omega_y/\sqrt{2})(\langle e|\hat{z}|g\rangle/\ell_B) \lesssim 10$ GHz is small compared to $h\nu_0 \simeq 140$ GHz and does not change the vertical dipole moment significantly. While the slope as a function of $E_\perp$ remains unchanged, an overall energy shift $\delta\epsilon$ is visible. It appears due to the coupling between Rydberg states and Landau levels at finite B_y. In the following, we present a careful experimental investigation

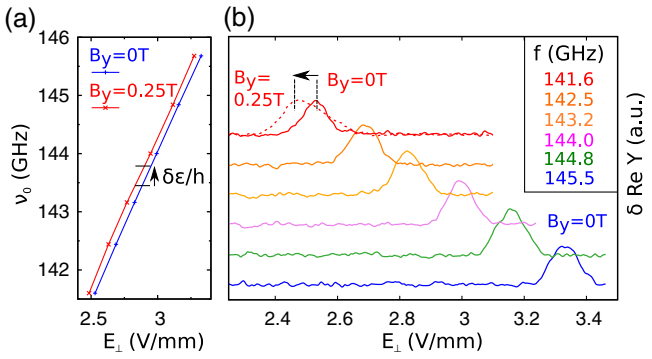

FIG. 2. (a) The shift of the $|g\rangle \to |e\rangle$ transition energy due to Stark effect at $B_z = 0.73$ T for $B_y = 0$ and $B_y = 0.25$ T. The slope is the same for both lines, but a small energy shift $\delta\epsilon$ is observed. (b) The Stark shift as seen from raw δY data at $B_y = 0$. The dashed line displays the shift of the resonance with B_y for $f = 141.6$ GHz, and $\delta\epsilon$ can also be deduced from the value of this Stark shift.

of the coupling-induced energy shift and show that it can be understood quantitatively from the QED Hamiltonian.

To study the evolution of the $|g\rangle \to |e\rangle$ transition with B_y, we take advantage of the linear dependence of the energy shifts on $E_\perp$, which enables us to fix the excitation frequency to $f = 139$ GHz and change only $E_\perp$. We define δ as the detuning induced by the Shark shift due to the deviation of $E_\perp$ from its resonant value at the excitation frequency f for $B_y = 0$; δ is thus the difference between $E_\perp$ and its value at resonance $\simeq 2V\text{mm}^{-1}$ times (minus) the slope measured in Fig. 2(a). All the collected data are then transformed into a map where the change in admittance is plotted as function of B_y and of the detuning δ. The maps that we obtained for $B_z = 1.3$ and 1.05 are displayed in Figs. 3(a) and 3(b). When increasing B_y, we can resolve two transitions Δ_0 and Δ_1. The energy of the more intense transition called Δ_0 increases with B_y, quadratically at weak B_y with a crossover to a more linear dependence at the highest fields. In addition to this main transition, a weaker transition Δ_1 splits off from the main transition as B_y becomes stronger. (As will be shown later, Δ_1 is visible only at the highest microwave excitation power, which was here fixed to its maximal value of 10 mW.) This Δ_1 transition becomes as visible as the main transition at lower B_z [Figs. 3(c) and 3(d) for $B_z = 0.85$ and 0.73 T] giving two mutually inverse curves with a characteristic "butterfly" pattern. The coupling strength dependence of Δ_0 is almost the same for all B_z in our dataset. On the contrary, for Δ_1, the slope of the transition line as a function of the coupling strength increases significantly with B_z.

The splitting of the Rydberg transition can be understood from the energy level diagram in Fig. 3(e), which shows how the energy levels from the QED Hamiltonian evolve with the coupling strength. For each atomic state $|\alpha\rangle$, the manifold of dressed states consists of a ladder of Landau levels $|\alpha, m\rangle$ with MW exciting transitions that conserve the Landau level number m (between states with the same number of photons in the cavity). Without a parallel magnetic field, the energy of the $|g, m\rangle \to |e, m\rangle$ transition is not dependent on m. The coupling lifts this degeneracy, making transitions associated with different Landau levels spectroscopically distinguishable. In the special case of the $m = 0$ transition $|g, 0\rangle \to |e, 0\rangle$ with energy Δ_0, the renormalization of the transition energy is due to an interaction with the lowest Landau level. It can be seen as an effective Lamb shift in analogy with atomic physics, circuit QED [42,43], and physics of electrons coupled to phonons or ripplons [44,45]. A similar renormalization occurs for all the transitions $|g, m\rangle \to |e, m\rangle$, and simulations are thus needed to identify the observed spectroscopic lines as one of the transitions Δ_m.

The QED Hamiltonian gives a quantitative prediction on the renormalization of the transition energies Δ_m. We emphasize that all the parameters appearing in the model involve $E_\perp$, the applied magnetic field, the liquid helium

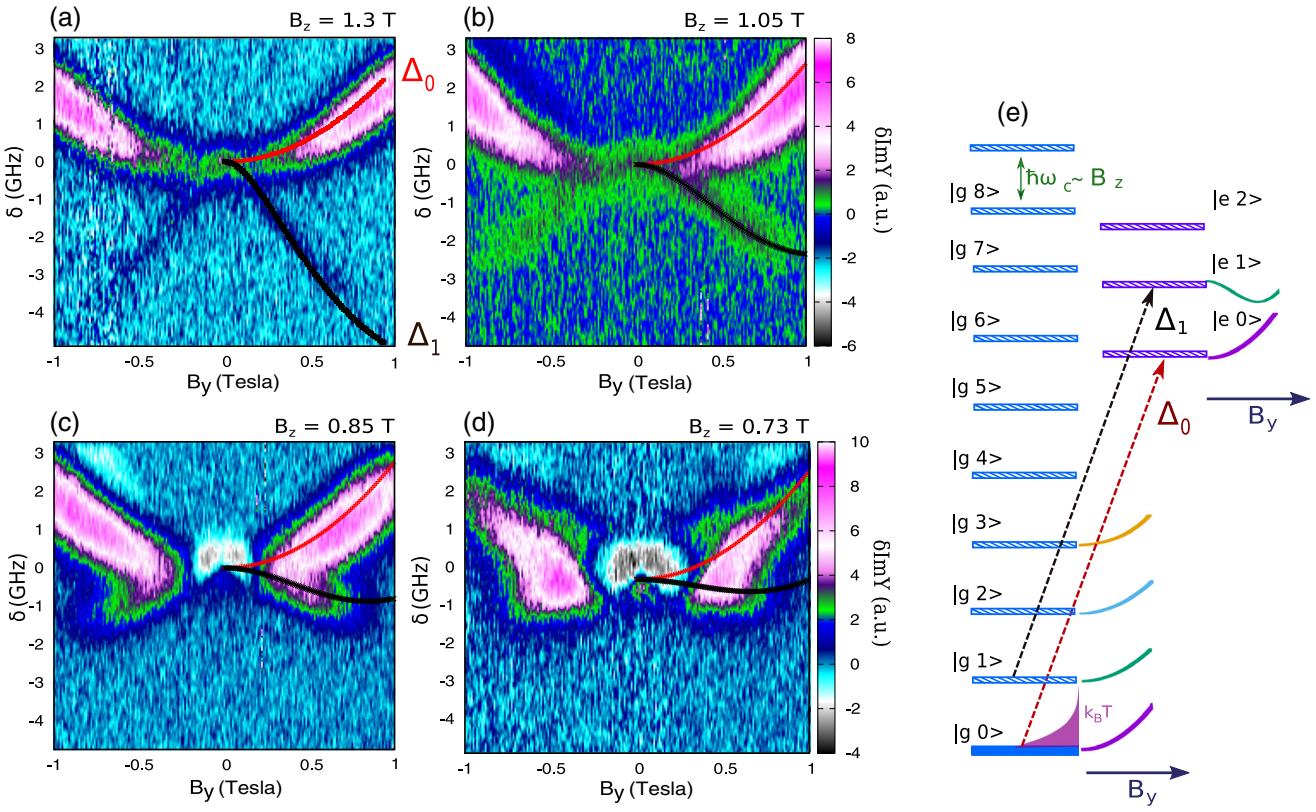

FIG. 3. Evolution of the $|g\rangle \rightarrow |e\rangle$ resonance with B_y showing that this resonance splits into two branches. The color maps represent δY as function of B_y and detuning δ for (a) $B_z = 1.3$, (b) 1.05, (c) 0.85, and (d) 0.73 T. Red and black curves give the QED Hamiltonian predictions for the Δ_0 and Δ_1 transitions drawn in (e) between states $|n, m\rangle$, where the first quantum number gives the atomic state and m is the Landau level number (number of photons in the cavity). The calculated evolution of individual levels (rescaled for visibility) with B_y up to 1 T is shown by colored lines.

dielectric constant ϵ, and fundamental constants, thus there are no fitting parameters. The values of Δ_m can be obtained from the numerical diagonalization of Eq. (2). To obtain accurate values, we had to include Rydberg states and Landau levels at an energy scale higher than $\hbar\nu_0$ from $|g, 0>$. In the simulations shown here, we used a basis set of 100 Landau levels and 20 Rydberg states. Results of our simulations for transitions $\Delta_{0,1}$ are overlaid on top of the experimental data. We see that they reproduce accurately both upper and lower "butterfly wings," including the striking increase of $\Delta_1(B_y)$ with B_z, which contrasts with the Δ_0 transition that is almost B_z independent.

The transitions Δ_m between states $|g, m\rangle \rightarrow |e, m\rangle$ can only be observed if the initial state $|g, m\rangle$ is populated. At the experiment temperature $T = 0.3$ K only the ground state $|g, 0\rangle$ is populated in equilibrium (the thermal population of $|g, 1\rangle$ at $T = 0.3$ K and $B_z = 1$ T is only 1%). As a consequence, the transitions Δ_m with $m \geq 1$ require an external excitation to become visible. In Fig. 4(a), we show that, indeed, these transitions physically appear only when the MW power is high enough, as opposed to the Δ_0 transition, which is present even at low MW power. Two possible mechanisms to populate the $|g, 1\rangle$ level may be taken into consideration. The first assumes an in-plane component of the MW electric field populating a $|g, 1\rangle$ level nonresonantly from the initial $|g, 0\rangle$ level. The second one is illustrated with dashed lines in Fig. 4(b). When the energy of the transitions $\Delta_{0,1}$ is sufficiently close (at

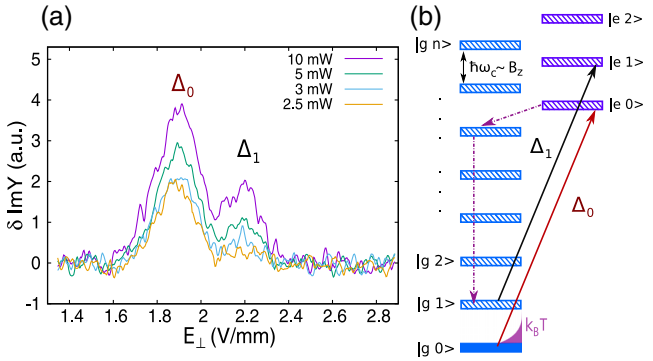

FIG. 4. (a) Dependence of the $\Delta_{0,1}$ resonances on MW excitation power at $B_z = 1$ T, $B_y = 0.5$ T. The Δ_1 transition disappears at low power. (b) Illustrates how the Δ_0 transition can populate the $|g, 1\rangle$ level. If the energies $\Delta_{0,1}$ are close, MW photons at the Δ_1 energy can also induce the Δ_0 transition, providing the nonequilibrium population needed to see the resonance at Δ_1.

low B_y), a Δ_1 energy MW photon can also excite a transition into the $|e,0\rangle$ state. Scattering can then transfer some population into a nearby $|g,m\rangle$ level, leading (after relaxation) to a finite population in the $|g,1\rangle$ state, which makes the transition Δ_1 visible. In Fig. 3 we see that, as B_y increases, the Δ_1 transition disappears faster than the Δ_0 transition. This observation can be understood within the population mechanism for $|g,1\rangle$ shown in Fig. 4(b). Indeed, at larger B_y, the energies of the $\Delta_{0,1}$ transitions become different and the MW excitation at the Δ_1 frequency can no longer excite the Δ_0 transition that populates the $|g,1\rangle$ level. The state $|g,1\rangle$ then remains empty, leading to the disappearance of the Δ_1 wings.

In conclusion, we have shown that 2DES on liquid helium can form a prototype quantum system of an atom coupled to an oscillator with the coupling directly controllable by the parallel magnetic field. Our spectroscopic results compare very accurately to theoretical predictions with no adjustable parameters. Control of the population transfer between dressed states could enable tunable millimeter-wave lasers, and future experiments at high electron densities may reveal a rich quantum many-body physics.

We acknowledge discussions with K. Kono, and D. L. Shepelyansky who stimulated these experiments, as well as support from N. Vernier, V. P. Dvornichenko, Okinawa Institute of Science and Technology (OIST) Graduate University, and ANR SPINEX.

[1] K. v. Klitzing, G. Dorda, and M. Pepper, Phys. Rev. Lett. **45**, 494 (1980).
[2] D. C. Tsui, H. L. Stormer, and A. C. Gossard, Phys. Rev. Lett. **48**, 1559 (1982).
[3] J. K. Jain, *Composite Fermions* (Cambridge University Press, Cambridge, England, 2007), p. 1225.
[4] K. Novoselov, A. Geim, S. Morozov, D. Jiang, M. Katsnelson, I. Grigorieva, S. Dubonos, and A. Firsov, Nature (London) **438**, 197 (2005).
[5] Y. Zhang, Y.-W. Tan, H. L. Stormer, and P. Kim, Nature (London) **438**, 201 (2005).
[6] M. König, S. Wiedmann, C. Brüne, A. Roth, H. Buhmann, L. W. Molenkamp, X.-L. Qi, and S.-C. Zhang, Science **318**, 766 (2007).
[7] R. Williams, R. S. Crandall, and A. H. Willis, Phys. Rev. Lett. **26**, 7 (1971).
[8] W. T. Sommer and D. J. Tanner, Phys. Rev. Lett. **27**, 1345 (1971).
[9] T. R. Brown and C. C. Grimes, Phys. Rev. Lett. **29**, 1233 (1972).
[10] C. C. Grimes, T. R. Brown, M. L. Burns, and C. L. Zipfel, Phys. Rev. B **13**, 140 (1976).
[11] K. Shirahama, S. Ito, and H. e. a. Suto, J. Low Temp. Phys. **101**, 439 (1995).
[12] C. C. Grimes and G. Adams, Phys. Rev. Lett. **42**, 795 (1979).
[13] D. S. Fisher, B. I. Halperin, and P. M. Platzman, Phys. Rev. Lett. **42**, 798 (1979).
[14] C. C. Grimes and G. Adams, Phys. Rev. Lett. **36**, 145 (1976).
[15] M. I. Dykman and L. S. Khazan, Sov. Phys. JETP **77**, 1488 (1979).
[16] M. I. Dykman, M. J. Lea, P. Fozooni, and J. Frost, Phys. Rev. Lett. **70**, 3975 (1993).
[17] D. Konstantinov, M. I. Dykman, M. J. Lea, Y. Monarkha, and K. Kono, Phys. Rev. Lett. **103**, 096801 (2009).
[18] H. Ikegami, H. Akimoto, D. G. Rees, and K. Kono, Phys. Rev. Lett. **109**, 236802 (2012).
[19] D. G. Rees, N. R. Beysengulov, J.-J. Lin, and K. Kono, Phys. Rev. Lett. **116**, 206801 (2016).
[20] P. M. Platzman and M. I. Dykman, Science **284**, 1967 (1999).
[21] D. I. Schuster, A. Fragner, M. I. Dykman, S. A. Lyon, and R. J. Schoelkopf, Phys. Rev. Lett. **105**, 040503 (2010).
[22] M. A. Zudov, R. R. Du, J. A. Simmons, and J. L. Reno, Phys. Rev. B **64**, 201311(R) (2001).
[23] P. Ye and L. Engel, Appl. Phys. Lett. **79**, 2193 (2001).
[24] R. G. Mani, A. N. Ramanayaka, and W. Wegscheider, Phys. Rev. B **84**, 085308 (2011).
[25] D. Konstantinov and K. Kono, Phys. Rev. Lett. **103**, 266808 (2009).
[26] Y. P. Monarkhaa, Low Temp. Phys. **37**, 655 (2011).
[27] R. G. Mani, J. H. Smet, K. von Klitzing, V. Narayanamurti, W. B. Johnson, and V. Umansky, Nature (London) **420**, 646 (2002).
[28] M. Zudov, R. Du, L. Pfeiffer, and K. West, Phys. Rev. Lett. **90**, 046807 (2003).
[29] D. Konstantinov and K. Kono, Phys. Rev. Lett. **105**, 226801 (2010).
[30] D. Konstantinov, A. Chepelianskii, and K. Kono, J. Phys. Soc. Jpn. **81**, 093601 (2012).
[31] A. D. Chepelianskii, M. Watanabe, K. Nasyedkin, K. Kono, and D. Konstantinov, Nat. Commun. **6**, 7210 (2015).
[32] Y. P. Monarkha, Low Temp. Phys. **42**, 441 (2016).
[33] S. Haroche, Rev. Mod. Phys. **85**, 1083 (2013).
[34] J. M. Fink, L. Steffen, P. Studer, L. S. Bishop, M. Baur, R. Bianchetti, D. Bozyigit, C. Lang, S. Filipp, P. J. Leek, and A. Wallraff, Phys. Rev. Lett. **105**, 163601 (2010).
[35] A. Bienfait, J. J. Pla, Y. Kubo, X. Zhou, M. Stern, C. C. Lo, C. D. Weis, T. Schenkel, D. Vion, D. Esteve, J. J. L. Morton, and P. Bertet, Nature (London) **531**, 74 (2016).
[36] E. Collin, W. Bailey, P. Fozooni, P. G. Frayne, P. Glasson, K. Harrabi, M. J. Lea, and G. Papageorgiou, Phys. Rev. Lett. **89**, 245301 (2002).
[37] T. M. Fromhold, L. Eaves, F. W. Sheard, M. L. Leadbeater, T. J. Foster, and P. C. Main, Phys. Rev. Lett. **72**, 2608 (1994).
[38] D. L. Shepelyansky and A. D. Stone, Phys. Rev. Lett. **74**, 2098 (1995).
[39] G. S. Boebinger, A. Passner, L. N. Pfeiffer, and K. W. West, Phys. Rev. B **43**, 12673 (1991).
[40] W. Mayer, J. Kanter, J. Shabani, S. Vitkalov, A. K. Bakarov, and A. A. Bykov, Phys. Rev. B **93**, 115309 (2016).
[41] W. Mayer, S. Vitkalov, and A. A. Bykov, Phys. Rev. B **96**, 045436 (2017).

[42] P. W. Milonni, *The Quantum Vacuum: An Introduction to Quantum Electrodynamics* (Academic Press, New York, 2013).

[43] A. Wallraff, D. I. Schuster, A. Blais, L. Frunzio, R.-S. Huang, J. Majer, S. Kumar, S. M. Girvin, and R. J. Schoelkopf, Nature (London) **431**, 162 (2004).

[44] A. J. Ramsay, T. M. Godden, S. J. Boyle, E. M. Gauger, A. Nazir, B. W. Lovett, A. M. Fox, and M. S. Skolnick, Phys. Rev. Lett. **105**, 177402 (2010).

[45] M. I. Dykman, K. Kono, D. Konstantinov, and M. J. Lea, Phys. Rev. Lett. **119**, 256802 (2017).